

## **Chapter 9 Test of electrodes based on manganese oxide with and without potassium cations for supercapacitors**

### **Capítulo 9 Prueba de electrodos a base de óxidos de manganeso con y sin cationes de potasio para supercapacitores**

CHÁVEZ-GÓMEZ, Karina del Carmen, LÓPEZ-LÓPEZ, Elizabeth and QUIROGA-GONZALEZ, Enrique\*

*Benemérita Universidad Autónoma de Puebla, Instituto de Física*

ID 1<sup>st</sup> Author: *Karina Del Carmen, Chávez-Gómez* / **ORC ID:** 0000-0003-2887-5864, **CVU CONAHCYT ID:** 629494

ID 1<sup>st</sup> Co-author: *Elizabeth, López-López* / **ORC ID:** 0009-0000-4984-6427

ID 2<sup>nd</sup> Co-author: *Enrique, Quiroga-Gonzalez* / **ORC ID** 0000-0003-1650-0862, **CVU CONAHCYT ID:** 48276

**DOI:** 10.35429/H.2023.6.90.96

K. Chávez, E. López, E. Quiroga

\*equiroga@ifuap.buap.mx.

S. Vargas, S. Figueroa, C. Patiño and J. Sierra (AA. VV.) Engineering and Applied Sciences. Handbooks-TI-©ECORFAN-Mexico, Mexico City, 2023

## Abstract

The demand for more efficient energy storage devices with a sustainable approach has turned supercapacitors into a great alternative in applications where high instantaneous power is required. Above all, those based on manganese oxides are attracting attention for their low cost, durability, and relatively high specific capacitance. However, it is known that  $\text{MnO}_2$  with a pyrolusite structure ( $\beta\text{-MnO}_2$ ) has a poor performance. This work studies this material electrochemically before and after thermally incorporating potassium cations at 800 °C. For the present work, commercial  $\text{MnO}_2$  and  $\text{MnO}_2$  doped with potassium ions ( $\text{K-MnO}_2$ ) were used as active material for the electrodes of commercial supercapacitors. It was verified that the commercial material is  $\beta\text{-MnO}_2$  and that the thermally doped material is predominantly manganese oxide with a cryptomelane structure ( $\alpha\text{-K}_x\text{MnO}_2$ ). Cyclic voltammetry measurements were performed at different scanning rates, to elucidate the electrochemical response of the materials. The results corresponding to  $\text{K-MnO}_2$  present a higher current compared to commercial  $\text{MnO}_2$ , this implies that this electrode has a higher specific capacitance, which can be attributed to a greater potassium ion insertion/extraction capacity. However, at high scanning speeds, its behavior shows that it is pseudocapacitive.

## Supercapacitors, Manganese oxide, Capacitance, Electrochemical tests

### Resumen

La demanda de dispositivos de almacenamiento de energía más eficientes y con enfoque sustentable, ha convertido a los supercapacitores en una gran alternativa en aplicaciones donde se requiere alta potencia instantánea. Sobre todo, están llamando la atención por su bajo costo, durabilidad y relativamente alta capacitancia específica los basados en óxidos de manganeso. Sin embargo, es conocido que el  $\text{MnO}_2$  con estructura pirolusita ( $\beta\text{-MnO}_2$ ) presenta un pobre rendimiento. En este trabajo se estudia electroquímicamente al  $\text{MnO}_2$  antes y después de incorporarle cationes de potasio térmicamente a 800 °C. Para el presente trabajo se empleó como material activo de electrodos de supercapacitores  $\text{MnO}_2$  comercial y  $\text{MnO}_2$  dopado con iones potasio ( $\text{K-MnO}_2$ ) de manera térmica. Se comprobó que el material comercial es  $\beta\text{-MnO}_2$  y que el material dopado térmicamente es predominantemente óxido de manganeso con estructura criptomelano ( $\alpha\text{-K}_x\text{MnO}_2$ ). Se realizaron mediciones de voltamperometría cíclica a diferentes velocidades de barrido, para dilucidar la respuesta electroquímica de los materiales. Los resultados correspondientes al  $\text{K-MnO}_2$  presentan una corriente mayor respecto a las del  $\text{MnO}_2$  comercial, esto implica que este electrodo tiene una capacitancia específica superior, la cual puede atribuirse a una mayor capacidad de inserción/extracción de iones potasio. Sin embargo, a velocidades altas de barrido, su comportamiento denota ser pseudocapacitivo.

## Supercapacitores, Óxido de manganeso, Capacitancia, Pruebas electroquímicas

### 1. Introduction

The constant development of electrical devices has led to an increasing demand for energy, and as a consequence an advance in energy storage devices (Paramati *et al.*, 2022). Energy is an essential factor for development and progress, so its supply and storage is of vital importance, especially in the process of decarbonization of the global economy, which is gradually taking place (Spinelli *et al.*, 2022). At present, the development of efficient, stable systems capable of providing energy storage with high power represents a major challenge. Supercapacitors stand out from other devices, due to high instantaneous power (they can supply large currents in a short time) and large number of charge/discharge cycles (Gonzalez *et al.*, 2016).

Given the characteristics already mentioned above, electrochemical capacitors are commonly used in short-term applications requiring high power (Khan *et al.*, 2023). Supercapacitors are increasingly being used for industrial applications as they compaginate with green energy (Mensah-Darkwa *et al.*, 2019). As they have the property of storing energy quickly.

The performance of supercapacitors can be evaluated in terms of electrochemical properties, which depend on the properties of the electrodes and the electrolyte (Vangari *et al.*, 2013). Various materials that can rapidly accumulate charge, which is the main characteristic of supercapacitors, have been tested. Initially, ruthenium dioxide (RuO<sub>2</sub>) was used as the electrode, obtaining a drastic decrease in the internal resistance that characterized the first supercapacitors, making them much more cost-effective and allowing their use as energy storage media in the field of automation (Zhang *et al.*, 2021), RuO<sub>2</sub> presents good specific capacitance properties; however, being a costly material with negative effects on the environment, alternatives have been sought in other metal oxides or combinations based on carbon and oxides, among which manganese dioxide (MnO<sub>2</sub>) stands out; above all, they are attracting attention for their low cost, durability and relatively high specific capacitance (Kour *et al.*, 2022).

Despite the good performance of MnO<sub>2</sub> as a charge store in a supercapacitor, few of its phases exhibit this performance (Sari *et al.*, 2017). In particular, the performance of the pyrolusite phase is very poor, around 9- 11F/g (Devaraj *et al.*, 2008; Pundir *et al.*, 2023). On the other hand, the birnesite phase, with specific capacitance of 230 F/g is among the best (Komaba *et al.*, 2008; Zhu *et al.*, 2020). This may be due to the fact that the structure of the latter phase contains mobile cations, and that the interatomic spacing allows it. In this work we intend to electrochemically study MnO<sub>2</sub> with pyrolusite structure before and after incorporating potassium cations thermally at 800 °C, to elucidate the effect of cation incorporation and structural change on the electrochemical performance.

## 2. Methodology

Commercial MnO<sub>2</sub> powders (Sigma-Aldrich) and MnO<sub>2</sub> doped with potassium ions (K-MnO<sub>2</sub>) were used for the present study.

### 2.1. Synthesis of K- MnO<sub>2</sub>

Commercial MnO<sub>2</sub> powders (Sigma-Aldrich) and potassium hydroxide (KOH) flakes, both in a 1:1 molar ratio, were used. The KOH flakes were first crushed in a crucible and then the MnO<sub>2</sub> powders were added. Heat treatment was carried out at 800 °C for 2 h at temperature and allowed to cool to room temperature. The powders obtained were washed with deionized water until a neutral pH was obtained, and then they could be used in the fabrication of the electrodes.

### 2.2. Characterization techniques

To identify the phase of the manganese oxides, the X-ray diffractometry (XRD) technique was used, using the Panalytical - Empyrean diffractometer. As part of the chemical analysis, a Raman microscope of the Horiba LabRAM brand was used, with a He-Ne laser (632.8 nm).

### 2.3. Electrode fabrication

The electrodes for the supercapacitors in the study were developed from a mixture of three components: manganese oxide (MnO<sub>2</sub> and K-MnO<sub>2</sub>), carbon black (CB) and polyvinylidene fluoride (PVDF). The weight ratio of the above materials was 70:20:10. The paste obtained was deposited on a T-316 stainless steel mesh (food grade) of 100 wires/inch wire gauge 49 (0.03mm) and mesh opening 0.033mm, which was used as a current collector substrate.

### 2.4. Electrochemical characterization

The cyclic voltammetry tests were performed in a Zahner Zennium potentiostat, using the software of the same Thales equipment for the analysis and acquisition of data, in a 3-electrode cell. The working electrode (WE) which is the paste electrode with the metal oxide to be studied (MnO<sub>2</sub>), a reference electrode (RE) of Ag/AgCl and the third one that closes the electrical circuit, called counter electrode (CE) of platinum, and 6 M potassium hydroxide (KOH) will be used as electrolyte. Measurements were performed in an operating window from -500 to 750 mV, using sweep speeds of 200, 100, 50, 50, 20, 10, 10, 5, 4, 3 and 2 mV/s.

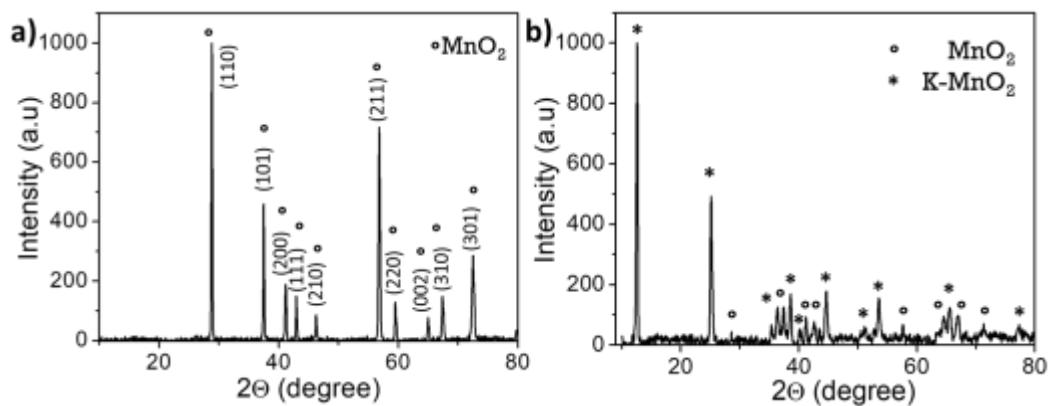
### 3. Results

The results obtained from the characterization and discussion of the manganese oxides, the commercial one which is the base material and the resulting oxide after cation insertion are shown below. In addition, the results of the electrochemical test assembled as an electrode in a supercapacitor are presented.

#### 3.1. XRD analysis of the manganese oxides

The structural characterization of the material was carried out by X-ray diffraction. Graph 3.1 shows the diffractograms corresponding to commercial MnO<sub>2</sub> and MnO<sub>2</sub> with thermal treatment and ion insertion. In graph 3.1a the diffraction peaks correspond to those characteristic of pyrolusite, planes (110), (101), (200), (111), (200), (111), (210), (211), (220), (002), (310) and (301) can be identified, they can be indexed to the tetragonal  $\beta$ -MnO<sub>2</sub> phase (JCPDS card N° 24-0735). No peaks for other phases are observed, indicating high purity and crystallinity in the sample. On the other hand, the diffractogram of graph 3.1b, presents diffraction peaks of 2 phases, one of them is of the  $\beta$ -MnO<sub>2</sub> as it is the precursor material still present after the thermal treatment and the second resulting phase coincides with the tetragonal phase of the cryptomelane  $\square$ -KxMnO<sub>2</sub> (JCPDS card N° 29-1020), identifying the planes (110), (200), (220), (310), (211), (520) and (431). Comparing the intensity of the highest reflections of the two phases present, qualitatively it is possible to say that this sample is predominantly  $\square$ -KxMnO<sub>2</sub>.

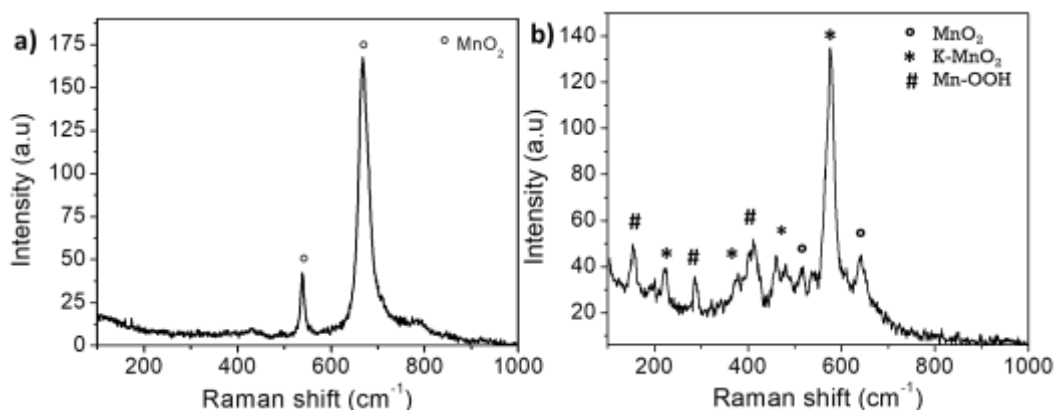
**Figure 3.1** XRD patterns corresponding to a) commercial MnO<sub>2</sub> and b) K-MnO<sub>2</sub>



#### 3.2. Characterization by Raman spectroscopy

The samples were analyzed by Raman spectroscopy, graph 3.2a corresponds to the commercial MnO<sub>2</sub>, it can be observed the well-defined characteristic bands at 557 cm<sup>-1</sup> and 668 cm<sup>-1</sup> of the  $\beta$ -MnO<sub>2</sub> phase. Graph 3.2b, belonging to the K-MnO<sub>2</sub> sample, shows the  $\beta$ -MnO<sub>2</sub> bands, in addition to the bands positioned at 185, 376 and 576 cm<sup>-1</sup> corresponding to  $\square$ -KxMnO<sub>2</sub>. In addition, of the synthesized phases that agree with the XRD results, bands appear at positions 157, 284 and 411 cm<sup>-1</sup> that can be indexed to the corresponding Mn-OOH phase.

**Figure 3.2** Raman spectra for a) commercial MnO<sub>2</sub> and b) K-MnO<sub>2</sub>

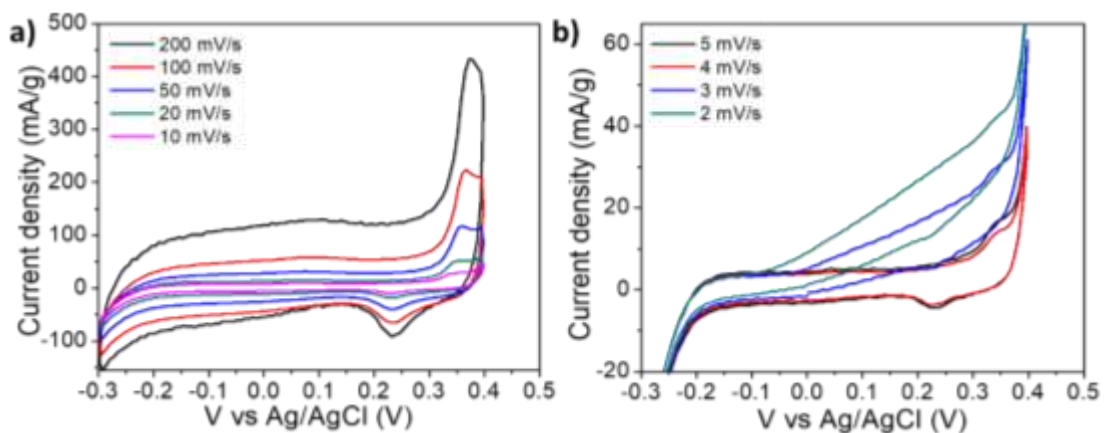


### 3.3 Caracterización electroquímica de los electrodos fabricados

Based on the characterization results, the  $\beta$ -MnO<sub>2</sub> was analyzed for the commercial manganese oxide and a mixture of  $\alpha$  and  $\beta$  phases for the oxide with potassium ion insertion. Voltammetry tests were performed on them in a KOH electrolyte.

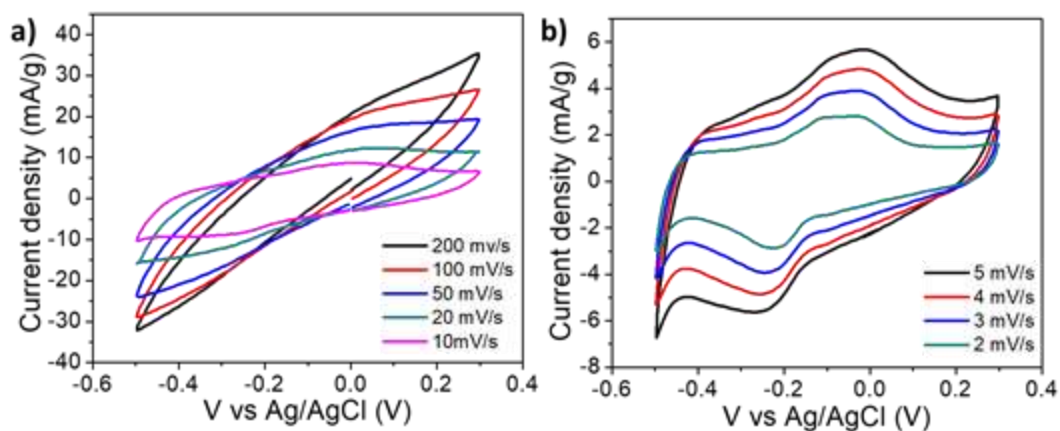
To understand the electrochemical behavior of the manganese oxides, they were tested as electrodes in supercapacitor in an aqueous medium, at different rates both fast and slow to observe at which rate the electrode obtains higher current density. Figure 3.3 shows the cyclic voltammetry curves for commercial MnO<sub>2</sub> at different sweep speeds. A pair of approximately symmetrical redox peaks can be observed in the CV curve at voltages 0.25 and 0.35 V, due to the intercalation/de-intercalation of protons or alkali metal ions on the MnO<sub>2</sub> electrode, confirming the pseudocapacitive characteristics. As the scan rate increases, the current intensity increases, while the position (x-axis) of the redox peak shifts only slightly, indicating a good electrochemical reversibility of the system, it is also observed in graph 3.3b that at low speeds the commercial MnO<sub>2</sub> loses the characteristic shape of its voltammogram and the oxidation and reduction peaks are not well defined.

**Figure 3.3** Cyclic voltammetry plots at a) fast scanning speeds and b) slow speeds of commercial MnO<sub>2</sub>



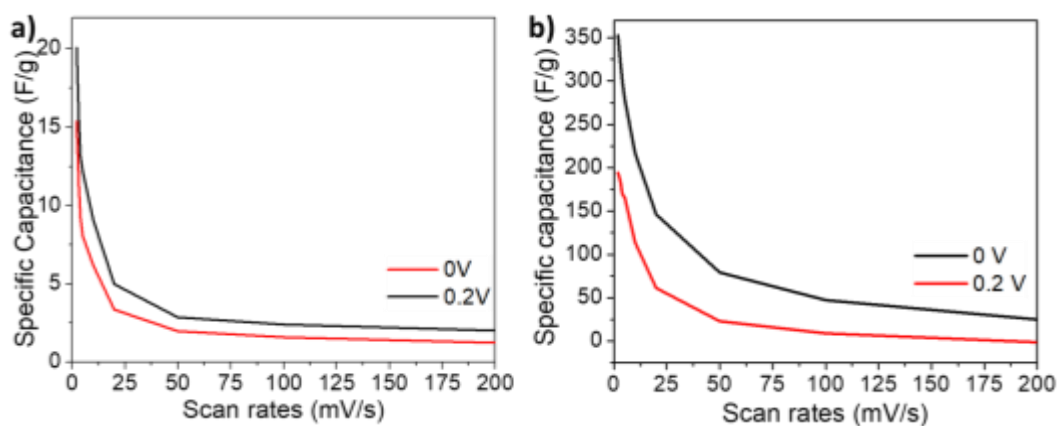
Cyclic voltammetry was performed to know the electrocatalytic activity of K-MnO<sub>2</sub> in 6 M KOH as electrolyte. Graph 3.4 shows the voltammograms obtained at different sweep speeds from 200 mV/s to 2 mV/s. The behavior of the cell with KOH electrolyte, a redox process is present with an oxidation peak at -0.04 V and a reduction peak at -0.24 V, but only at low sweep speeds. In addition, comparing the current values of K-MnO<sub>2</sub> with respect to those in graph 3.3, a considerable increase is observed, thus proving that the insertion of K ions in the composite acts favorably to increase the current density in the electrode.

**Figure 3.4** Cyclic voltammetry plots at a) fast scanning speeds and b) slow K-MnO<sub>2</sub> speeds



Graph 3.5 shows the specific capacitance of the MnO<sub>2</sub> and K-MnO<sub>2</sub> electrode as a function of the sweep speed at 2 different potentials 0 and 0.2 V, the specific capacitances of the electrodes composed of MnO<sub>2</sub> were calculated from cyclic voltammetry data at different speeds, the capacitance values were measured at potentials where a faradaic process is observed and another in a capacitive part, also shows the behavior of the capacitance at different sweep speeds, noting that the higher the sweep speed the specific capacitance decreases, this is due to insufficient time for the ions to diffuse into the electrode material (Thomas *et al.*, 2023). In contrast, better storage capacitance is favorable at lower scan rates because slow ionic propagation in the electrolyte-electrode can improve its chemical reactivity. One can compare the capacitance we obtain from MnO<sub>2</sub> and K-MnO<sub>2</sub>, at a rate of 2 mV/s for MnO<sub>2</sub> it is 20 F/g, while for K-MnO<sub>2</sub> at the same rate it is 350 F/g (17 times higher). This is attributed to the incorporation of K<sup>+</sup> cations into the MnO<sub>2</sub> structure by heat treatment, which enhances the ion insertion/extraction capacity of the material. At fast rates the capacitance tends to stabilize at one value, indicating pseudocapacitive behavior (Jones *et al.*, 2023). It has been shown that the addition of ions makes the charge storage mechanisms more surface redox dominated and can improve the specific capacitance (Barclay *et al.*, 2023).

**Graph 3.5** Comparative graph of the specific capacitances vs. sweep speeds of a)  $\beta$ -MnO<sub>2</sub> and b) K-MnO<sub>2</sub>



#### 4. Conclusions

From the voltammetry curves it can be seen that the K-MnO<sub>2</sub> graphs present a higher current density with respect to that of commercial MnO<sub>2</sub>. The incorporation of ions in the structure of the material with the thermal treatment, allows the insertion and extraction of ions in an electrochemical way when using it as an electrode of supercapacitors. When analyzing the specific capacitance graphs, it is observed that at fast speeds the capacitance decreases exponentially, but tends to stabilize at fast speeds. This is an indication that at slow speeds the storage process is diffusion limited, and at fast speeds it is pseudocapacitive. Although the K-MnO<sub>2</sub> material is not a pure phase, and the potassium phase is cryptomelane (a phase with low cation content), its response as an electrochemical energy store is vastly superior (17 times higher gravimetric capacitance) to commercial MnO<sub>2</sub> with pyrolusite structure.

#### References

- Barclay, M., et al. (2023). Plasma-activated water for improved intercalation and pseudocapacitance of MnO<sub>2</sub> supercapacitor electrodes. *Materials Today Sustainability*, 22, 100388. doi:<https://doi.org/10.1016/j.mtsust.2023.100388>
- Devaraj, S., & Munichandraiah, N. (2008). Effect of Crystallographic Structure of MnO<sub>2</sub> on Its Electrochemical Capacitance Properties. *The Journal of Physical Chemistry C*, 112(11), 4406-4417. doi:<https://doi.org/10.1021/jp7108785>
- González, A., et al. (2016). Review on supercapacitors: Technologies and materials. *Renewable and Sustainable Energy Reviews*, 58, 1189-1206. doi: <https://doi.org/10.1016/j.rser.2015.12.249>

- Jones, D. R., et al. (2023). Scalable Synthesis of Pre-Intercalated Manganese(III/IV) Oxide Nanostructures for Supercapacitor Electrodes: Electrochemical Comparison of Birnessite and Cryptomelane Products. *ChemElectroChem*, 10(14), e202300210. doi:<https://doi.org/10.1002/celec.202300210>
- Khan, M. S., et al. (2023). Unveiling the electrochemical advantages of a scalable and novel aniline-derived polybenzoxazole-reduced graphene oxide composite decorated with manganese oxide nanoparticles for supercapacitor applications. *Journal of Energy Storage*, 73, 109109. doi:<https://doi.org/10.1016/j.est.2023.109109>
- Komaba, S., Ogata, A., & Tsuchikawa, T. (2008). Enhanced supercapacitive behaviors of birnessite. *Electrochemistry Communications*, 10(10), 1435-1437. doi:<https://doi.org/10.1016/j.elecom.2008.07.025>
- Kour, S., Tanwar, S., & Sharma, A. (2022). A review on challenges to remedies of MnO<sub>2</sub> based transition-metal oxide, hydroxide, and layered double hydroxide composites for supercapacitor applications. *Materials Today Communications*, 104033. doi:<https://doi.org/10.1016/j.mtcomm.2022.104033>
- Mensah-Darkwa, K., et al. (2019). Supercapacitor energy storage device using biowastes: A sustainable approach to green energy. *Sustainability*, 11(2), 414. doi:<https://doi.org/10.3390/su11020414>.
- Paramati, S. R., Shahzad, U., & Doğan, B. (2022). The role of environmental technology for energy demand and energy efficiency: Evidence from OECD countries. *Renewable and Sustainable Energy Reviews*, 153, 111735. doi:<https://doi.org/10.1016/j.rser.2021.111735>.
- Pundir, S., et al. (2023). Synthesis of 1D  $\beta$ -MnO<sub>2</sub> for high-performance supercapacitor application. *Journal of Solid State Electrochemistry*, 27(2), 531-538. doi:<https://doi.org/10.1007/s10008-022-05347-z>.
- Sari, F. N. I., So, P. R., & Ting, J. M. (2017). MnO<sub>2</sub> with controlled phase for use in supercapacitors. *Journal of the American Ceramic Society*, 100(4), 1642-1652. doi:<https://doi.org/10.1111/jace.14636>.
- Spinelli, F., et al. (2022). Shipping Decarbonization: An Overview of the Different Stern Hydrodynamic Energy Saving Devices. *Journal of Marine Science and Engineering*, 10(5), 574. doi:<https://doi.org/10.3390/jmse10050574>.
- Thomas, M., et al. (2023). Nanoarchitectonics of high-performance supercapacitors based on mesoporous carbon and MnO<sub>2</sub> electrodes using Aquivion electrolyte membrane. *Journal of Alloys and Compounds*, 960, 170719. doi:<https://doi.org/10.1016/j.jallcom.2023.170719>
- Vangari, M., Pryor, T., & Jiang, L. (2013). Supercapacitors: review of materials and fabrication methods. *Journal of energy engineering*, 139(2), 72-79. doi:[https://doi.org/10.1061/\(ASCE\)EY.1943-7897.0000102](https://doi.org/10.1061/(ASCE)EY.1943-7897.0000102).
- Zhang, Q., et al. (2021). Energy release from RuO<sub>2</sub>//RuO<sub>2</sub> supercapacitors under dynamic discharge conditions. *Electrochimica Acta*, 367, 137455. doi:<https://doi.org/10.1016/j.electacta.2020.137455>.
- Zhu, S., et al. (2020). Birnessite based nanostructures for supercapacitors: challenges, strategies and prospects. *Nanoscale Advances*, 2(1), 37-54. doi: <https://doi.org/10.1039/C9NA00547A>.